Available online at www.sciencedirect.com
SCIENCE DIRECT®
PERGAMON
International Journal of Heat and Mass Transfer 46 (2003) 4235–4244
International Journal of HEAT and MASS TRANSFER
www.elsevier.com/locate/ijhmt

A lattice Boltzmann model for electrokinetic microchannel flow of electrolyte solution in the presence of external forces with the Poisson–Boltzmann equation

Baoming Li, Daniel Y. Kwok *

Nanoscale Technology and Engineering Laboratory, Department of Mechanical Engineering, The University of Alberta, 4-9 Mechanical Engineering, Edmonton, Alta., Canada T6G 2G8

Received 22 August 2002; received in revised form 17 April 2003

Abstract

Microchannel flow with electrolyte solution is often influenced by the presence of a double layer of electrical charges at the interface between the liquid and the wall of a substrate. These surface interactions affect strongly the physical and chemical properties of fluid and substantially influence the heat, mass and momentum transport in microfluidic systems. Traditional computational fluid dynamics methods using the modified Navier–Stokes equation for electrokinetics in solving macroscopic hydrodynamic equations have many difficulties in this area. We present here a lattice Boltzmann model in the presence of external force fields to describe electrokinetic microfluidic phenomena using a Poisson–Boltzmann equation. Pressure is considered as the only external force to drive liquid flow in microchannels. Our results from a 9-bit square lattice Boltzmann model are in excellent agreement with recent experimental data in pressure-driven microchannel flow that could not be fully described by electrokinetic theory. The differences between the predicted and experimental Reynolds numbers from pressure gradients are well within 5%. Our results suggest that the lattice Boltzmann model described here is an effective computational tool to predict the more complex microfluidic systems that might be problematic using conventional methods.

Keywords: Lattice Boltzmann model; Microchannel flow; Electrokinetics; Electrical double layer; Microfluidics

1. Introduction

Microchannel flow with electrolyte solution is often influenced by the presence of a double layer of electrical charges at the interface between the liquid and the wall of a substrate. This double layer is also known as the electrical double layer (EDL), causing the development of a streaming potential when a pressure gradient is applied to drive the flow or electroosmosis when an electric field is applied. Applications where such phenomena play an important role are in cooling of microelectronics [1–3], lab-on-a-chip diagnostic devices [4] and in vivo drug delivery systems [5,6].

As for the electrokinetic phenomena in general, electrically neutral liquids have a distribution of electrical charges near a surface because of a charged solid surface. This region is known as the EDL, which induces electrokinetic phenomena. The effect of EDL during an externally applied pressure gradient is to retard liquid flow, resulting in a streaming potential; whereas, in the absence of an external pressure gradient, EDL induces fluid flow when an external electric field is applied (electroosmotic pumping). EDL is primarily a surface phenomenon; its effects tend to appear when the typical dimension of channel is of the same order as the EDL thickness [7–12]. However, modeling of microfluidics has not been an easy task because of the inherent

* Corresponding author. Tel.: +1-780-492-2791; fax: +1-780-492-2200.
E-mail address: daniel.y.kwok@ualberta.ca (D.Y. Kwok).

0017-9310/$ - see front matter © 2003 Elsevier Ltd. All rights reserved.
doi:10.1016/S0017-9310(03)00218-7

complexity of surface and electrokinetic phenomena on flow characteristics. These surface interactions affect strongly the physical and chemical properties of fluid [13,14] and substantially influence the heat, mass and momentum transport in microfluidic systems [7,15–19]. In addition, traditional computational fluid dynamics methods using the modified Navier–Stokes equation for electrokinetics in solving macroscopic hydrodynamic equations have many difficulties in this area. Since the complexity of many fluid systems is essentially due to the microscopic interparticle interaction, lattice Boltzmann simulation provides an excellent alternative to model such complex fluid dynamics problems [20]. In recent years, the lattice Boltzmann method has attracted tremendous attention as an alternative to solve complex fluid dynamics problems. In particular, its simplicity of programming, parallelism of the approach, and the capability of incorporating microscopic interactions have been very attractive. Although the approach is based on microscopic interactions, all macroscopic continuum equations such as the Navier–Stokes equation can be derived and recovered.

In the lattice Boltzmann method, space is divided into a regular lattice. Each lattice point has an assigned set of velocity vectors with specified magnitudes and directions connecting the lattice point to its neighboring lattice points. The total velocity and fluid density are defined by specifying the amount of fluid associated with each of the velocity vectors. The fluid distribution function evolves at each time step through a two-step procedure. The first step is to advance the fluid particles to the next lattice site along their directions of motion. The second step is to simulate particle collisions by relaxing the distribution toward an equilibrium distribution using a linear relaxation parameter.

The lattice Boltzmann equation (LBE) has been demonstrated to be an effective computational tool for a broad variety of complex physical systems, including hydrodynamic system [21–28], magnetohydrodynamic systems [29] and multiphase and multicomponent fluids systems [30–33]. It has been shown [34–41] that the LBE can be directly derived from the continuous Boltzmann equation discretized in some special manner in both time and phase space; the LBE is simply a finite-difference form of the continuous Boltzmann equation. Most of the applications that have been performed in the past with lattice Boltzmann are for isothermal systems, due to the lack of a general purpose energy model. Although the LBE can be established on a solid theoretical foundation, some approximations are required in order to obtain the evolution equation of the distribution function $f(x,\xi,t)$ with discrete time and the equilibrium distribution function $f^{eq}(x,\xi,t)$ for the LBE model. For example, to use pressure P as an independent variable in the incompressible Navier–Stokes equation for microfluidics, it is necessary to introduce a local pressure distribution function. These approximations lead to certain limitations for practical application of the LBE. As an example, the lattice Boltzmann method is only applicable to low Mach number hydrodynamics, because a small velocity expansion is used in the derivation of Navier–Stokes equation from the LBE [42].

In the present work, we employed an equilibrium distribution function in the presence of external forces and derived the LBE with an additional (external) force term for microfluidics of electrolyte solution. These external forces can include the externally applied pressure and the Lorentz force associated with any externally applied electric and magnetic fields, internally smoothed electric and magnetic fields due to the motion of charged particles in space, and the equivalent force field due to intermolecular attraction. Discretization of our velocity space ensures that Navier–Stokes equation can be obtained at a macroscopic level. Because of the large dimension of microchannel relative to the lattice size, the primary focus of the lattice Boltzmann simulation appropriate for modeling fluids in the microscale regime is on the structure and dynamical properties of fluids near the fluid-solid interface, such as the effect of wettability on wall slip. Our derived lattice Boltzmann model will be applied to simulate a series of microfluidic systems with electrokinetic phenomena.

2. Lattice Boltzmann theory in the presence of external forces

2.1. Discretization of time

We start from the following continuous Boltzmann equation using a single-relaxation-time approximation as a collision model,

$$\frac{\partial f}{\partial t}+\xi\cdot\nabla f+F\cdot\nabla_{\xi}f=-\frac{f-f^{eq}}{\lambda} \tag{1}$$

where $f\equiv f(x,\xi,t)$ is the single-particle distribution function in the phase space (x,ξ), and ξ is the microscopic velocity. F is an external force vector which can depend on both space and time, λ is the relaxation time due to collision, and f^{eq} is an equilibrium distribution function. A fluid under steady state conditions, immersed in a conservative force field, is characterized by a distribution function that differs from the Maxwell-Boltzmann distribution by an exponential factor, known as the Boltzmann factor:

$$f^{eq}=\frac{\rho}{(2\pi RT)^{D/2}}\exp\left(-\frac{U(x)}{k_{B}T}\right)\exp\left(-\frac{(\xi-u)^{2}}{2RT}\right) \tag{2}$$

where $U(x)$ is the potential energy of conservative force field, R and D are the gas constant and dimension of

space, respectively. The macroscopic density ρ, velocity u, and temperature T are calculated as the moments of the distribution function:

$$\begin{aligned}\rho &= \int f \,\mathrm{d}\xi \\ \rho u &= \int \xi f \,\mathrm{d}\xi \\ \frac{D_0}{2}\rho RT &= \frac{1}{2}\int (\xi - u)^2 f \,\mathrm{d}\xi\end{aligned} \tag{3}$$

where D_0 is the number of degrees of freedom of a particle. He et al. [41] proposed a heuristic approach to model the interaction between fluid particles as an external force in the Boltzmann equation using a mean-field approximation. This approach involved the approximation, without proof, of substituting the distribution function in the force term (Eq. (1)) with its equilibrium value, e.g., the local Maxwellian distribution. It should be noted that $F \cdot \nabla_\xi f$ is identical to $F \cdot \nabla_\xi f^{\mathrm{eq}}$ up to second order because the first two Hermite coefficients of the distribution function are always the same as those in the local Maxwellian distribution. We assume

$$\nabla_\xi f \approx \nabla_\xi f^{\mathrm{eq}} = -\frac{\xi - u}{RT} f^{\mathrm{eq}} \tag{4}$$

Consequently, we obtain

$$\frac{\partial f}{\partial t} + \xi \cdot \nabla f + \frac{1}{\lambda} f = \left(\frac{1}{\lambda} + \frac{F \cdot (\xi - u)}{RT}\right) f^{\mathrm{eq}} \tag{5}$$

Eq. (5) can be formally rewritten in the form of an ordinary differential equation:

$$\frac{\mathrm{d}f}{\mathrm{d}t} + \frac{1}{\lambda} f = \frac{1}{\lambda'} f^{\mathrm{eq}} \tag{6}$$

$$\text{where } \frac{\mathrm{d}}{\mathrm{d}t} \equiv \frac{\partial}{\partial t} + \xi \cdot \nabla \tag{7}$$

is the time derivative along the characteristic line ξ.

$$\frac{1}{\lambda'} = \frac{1}{\lambda} + \frac{F \cdot (\xi - u)}{RT} \tag{8}$$

is the reciprocal of equivalent relaxation time due to external force. The above inhomogeneous ordinary differential equation can be formally integrated over a small time step of δ_t:

$$\begin{aligned} f(x + \xi\delta_t, \xi, t + \delta_t) &= \exp\left(-\frac{\delta_t}{\lambda}\right) \int_0^{\delta_t} \frac{1}{\lambda'} \exp\left(\frac{t'}{\lambda}\right) f^{\mathrm{eq}}(x + \xi t', \xi, t + t') \,\mathrm{d}t' \\ &\quad + \exp\left(-\frac{\delta_t}{\lambda}\right) f(x, \xi, t) \end{aligned} \tag{9}$$

Assuming that δ_t is small enough and f^{eq} is smooth enough locally, the following first order approximation can be made:

$$\begin{aligned} f^{\mathrm{eq}}(x + \xi t', \xi, t + t') &= f^{\mathrm{eq}}(x, \xi, t) + \frac{t'}{\delta_t}\{f^{\mathrm{eq}}(x + \xi\delta_t, \xi, t + \delta_t) - f^{\mathrm{eq}}(x, \xi, t)\} \\ &\quad + \mathrm{O}(\delta_t^2) \quad t' \in [0, \delta_t] \end{aligned} \tag{10}$$

With this approximation, Eq. (9) becomes

$$\begin{aligned} f(x + \xi\delta_t, \xi, t + \delta_t) &= \frac{1}{\lambda'} \exp\left(-\frac{\delta_t}{\lambda}\right) \left\{ \lambda \left(\exp\left(\frac{\delta_t}{\lambda}\right) - 1 \right) f^{\mathrm{eq}}(x, \xi, t) \right. \\ &\quad + \frac{\lambda^2}{\delta_t} \left(\left(\frac{\delta_t}{\lambda} - 1\right) \exp\left(\frac{\delta_t}{\lambda}\right) + 1 \right) (f^{\mathrm{eq}}(x + \xi\delta_t, \xi, \\ &\quad \left. t + \delta_t) - f^{\mathrm{eq}}(x, \xi, t)) \right\} + \exp\left(-\frac{\delta_t}{\lambda}\right) f(x, \xi, t) \end{aligned} \tag{11}$$

If we expand $\exp(-\delta_t/\lambda)$ in its Taylor expansion and, further, neglect the terms of order $\mathrm{O}(\delta_t^2)$ or smaller on the right-hand side of Eq. (11), then Eq. (11) becomes

$$\begin{aligned} f(x + \xi\delta_t, \xi, t + \delta_t) - f(x, \xi, t) &= -\frac{1}{\tau}\left(f(x, \xi, t) - \frac{\lambda}{\lambda'} f^{\mathrm{eq}}(x, \xi, t) \right) \end{aligned} \tag{12}$$

where $\tau \equiv \lambda/\delta_t$ is a dimensionless relaxation time. Eq. (12) is the evolution equation of the distribution function $f(x, \xi, t)$ with discrete time.

2.2. Hydrodynamic moments

Although f^{eq} is written as an explicit function of t, the time dependence of f^{eq} lies solely in the hydrodynamic variables ρ, u, and T; that is, $f^{\mathrm{eq}}(x, \xi, t) = f^{\mathrm{eq}}(x, \xi, \rho, u, T)$. Therefore, one must first compute ρ, u, and T before constructing the equilibrium distribution function, f^{eq}. Thus, the calculation of ρ, u, and T becomes one of the most crucial steps in discretizing the Boltzmann equation.

In order to numerically evaluate the hydrodynamic moments of Eq. (3), appropriate discretization in momentum space ξ must be accomplished; that is

$$\int \psi(\xi) f(x, \xi, t) \,\mathrm{d}\xi = \sum_\alpha W_\alpha \psi(\xi_\alpha) f^{\mathrm{eq}}(x, \xi_\alpha, t) \tag{13}$$

where $\psi(\xi)$ is a polynomial of ξ, W_α is a weighted coefficient of the quadrature, and ξ_α is the discrete velocity set or the abscissas of the quadrature. Accordingly, the hydrodynamic moments of Eq. (3) can be computed by

$$\begin{aligned} \rho &= \sum_\alpha f_\alpha \\ \rho u &= \sum_\alpha \xi_\alpha f_\alpha \\ \rho\epsilon &= \frac{1}{2}\sum_\alpha (\xi_\alpha - u)^2 f_\alpha \\ f_\alpha &\equiv f_\alpha(x, t) \equiv W_\alpha f(x, \xi_\alpha, t) \\ \epsilon &= \frac{D_0}{2} RT \end{aligned} \tag{14}$$

2.3. External force terms

In the simplified Boltzmann equation (5), F is the external force experienced by each particle. A very useful approximation to describe the dynamics of a fluid is to consider the motions of fluid particles that are governed by applied external fields with the macroscopic averaged internal fields, and smoothed in space and time due to the motion of all fluid particles. The external force terms can be expressed as

$$F = F_{\text{ext}} + q_\alpha(E_{\text{int}} + \xi \times B_{\text{int}}) + F_V \tag{15}$$

where F_{ext} represents the external forces, including the externally applied pressure and the Lorentz force associated with any externally applied electric and magnetic fields, E_{int} and B_{int} are, respectively, internally smoothed electric and magnetic fields due to the motion of all charged particles inside the fluid (e.g., the space charge in the microfluidics), and F_V is a single equivalent force due to intermolecular attraction. In biochips or lab-on-a-chip devices, water is usually used as the medium for a buffer solution. Here, we employ a potential energy function $V(R)$ of water to treat the intermolecular attraction. A large number of hypothetical models for water have been developed in order to discover the structure of water. These models involve orienting electrostatic effects and Lennard-Jones sites which may or may not coincide with one or more of the charged sites. The Lennard-Jones interaction accounts for the size of the molecules. It is repulsive at short distances, ensuring that the structure does not completely collapse due to electrostatic interactions. At intermediate distances it is significantly attractive but non-directional and competes with the directional attractive electrostatic interaction. The potential energy function considered here involve a rigid water monomer that is represented by three interaction sites with positive charges on the hydrogens and a negative charge on oxygen. The Coulombic interactions between all intermolecular pairs of charges along with a single Lennard-Jones term between oxygens determine the dimerization energy $V(R)$ for monomers m and n as given by Eq. (16)

$$V(R) = \sum_{i,j} \frac{q_i q_j e^2}{\epsilon_r \epsilon_0 r_{ij}(R)} + \frac{A}{(r_{ij}(R))^{12}} - \frac{B}{(r_{ij}(R))^6} \tag{16}$$

The parameters q_i, q_j, A, and B can be chosen to yield reasonable structural and energetic results for liquid water. It should be stressed in the framework of the present derivation that anisotropy is a consequence of an inappropriate intermolecular interaction. A single equivalent force field due to intermolecular attraction yield

$$F_V = -\nabla V(R) \tag{17}$$

2.4. Derivation of the lattice Boltzmann equation and its equilibrium distribution function in two-dimensional space

The LBE has the following ingredients: (1) an evolution equation, in the form of Eq. (12) with discretized time and phase space in which configuration space is of a lattice structure and momentum space is reduced to a small set of discrete momenta; (2) conservation constraints in the form of the hydrodynamic moments; (3) a proper equilibrium distribution function which leads to the Navier–Stokes equations. In what follows, the low Mach number expansion is first applied to the Maxwell-Boltzmann distribution function by an Boltzmann factor. In the LBEs, the equilibrium distribution function $f^{\text{eq}}(x, \xi, t)$ is obtained by a truncated small velocity expansion.

$$f^{\text{eq}}(x,\xi,t) = \frac{\rho}{(2\pi RT)^{D/2}} \exp\left(-\frac{U(x)}{RT}\right) \exp\left(-\frac{\xi^2}{2RT}\right) \times \left[1 + \frac{\xi \cdot u}{RT} + \frac{(\xi \cdot u)^2}{2(RT)^2} - \frac{u^2}{2RT}\right] + \mathrm{O}(u^3) \tag{18}$$

Calculating the hydrodynamic moments of f^{eq} is equivalent to evaluating the following integral in general:

$$\begin{aligned} I &= \int \psi(\xi) f^{\text{eq}} \, \mathrm{d}\xi \\ &= \frac{\rho}{(2\pi RT)^{D/2}} \exp\left(-\frac{U(x)}{k_B T}\right) \int \psi(\xi) \exp\left(-\frac{\xi^2}{2RT}\right) \\ &\quad \times \left[1 + \frac{\xi \cdot u}{RT} + \frac{(\xi \cdot u)^2}{2(RT)^2} - \frac{u^2}{2RT}\right] \mathrm{d}\xi \end{aligned} \tag{19}$$

The discretization of the 9-bit lattice single-relaxation-time model can be found elsewhere [36,42].

Employing the notation of the 9-bit discrete velocities and the weighted coefficients ω_α, we obtained the equilibrium function for the 9-bit LBE model as

$$f_\alpha^{\text{eq}} = \omega_\alpha \rho \exp\left(-\frac{U(x)}{k_B T}\right) \left[1 + \frac{3(e_\alpha \cdot u)}{c^2} + \frac{9(e_\alpha \cdot u)^2}{2c^4} - \frac{3u^2}{2c^2}\right] \tag{20}$$

where

$$e_\alpha = \begin{cases} (0,0) & \alpha = 0 \\ \left(\cos\left[\frac{\pi(\alpha-1)}{2}\right], \sin\left[\frac{\pi(\alpha-1)}{2}\right]\right)c & \alpha = 1,2,3,4 \\ \left(\cos\left[\frac{\pi(\alpha-5)}{2} + \frac{\pi}{4}\right], \sin\left[\frac{\pi(\alpha-5)}{2} + \frac{\pi}{4}\right]\right)\sqrt{2c} & \alpha = 5,6,7,8 \end{cases} \tag{21}$$

and $\omega_\alpha = 4/9$ for $\alpha = 0$, 1/9 for $\alpha = 1$–4, and 1/36 for $\alpha = 5$–8; $c = \delta_x/\delta_t$, and δ_x and δ_t are the lattice constant and time step size, respectively.

The evolution equation (12) of f can be written as

$$f_\alpha(x + e_\alpha\delta_t, t + \delta_t) - f_\alpha(x,t) = -\frac{1}{\tau}\left\{f_\alpha(x,t) - \left(1 + 3\tau\frac{\delta_t^2}{\delta_x}\frac{(e_\alpha - u)\cdot F}{c}\right)f_\alpha^{\mathrm{eq}}\right\} \quad (22)$$

3. Results and discussion

3.1. Analytic solution of pressure-driven liquid flow through microchannel in the presence of the electrical double layer

In this section, we use the square 9-bit lattice single-relaxation-time model in the presence of a conservative force field. As mentioned above, the 9-bit lattice single-relaxation-time is on a square lattice space with three speeds: 0, c, and $\sqrt{2}c$, where $c = \delta_x/\delta_t$, and δ_x and δ_t are the lattice constant and step size in time, respectively. The evolution equation (12) of the system can be simplified as

$$f_\alpha(x + e_\alpha\delta_t, t + \delta_t) - f_\alpha(x,t) = -\frac{1}{\tau}\left\{f_\alpha(x,t) - f_\alpha^{\mathrm{eq}}(\rho,u)\right\} + \frac{\delta_t^2}{\delta_x}g_\alpha \quad (23)$$

where the body force term g_α is given by

$$g_\alpha = \begin{cases} 0 & \alpha = 0 \\ \dfrac{1}{3c}\exp\left(-\dfrac{U(x)}{k_{\mathrm{B}}T}\right)e_\alpha\cdot F & \alpha = 1,2,3,4 \\ \dfrac{1}{12c}\exp\left(-\dfrac{U(x)}{k_{\mathrm{B}}T}\right)e_\alpha\cdot F & \alpha = 5,6,7,8 \end{cases} \quad (24)$$

The Navier–Stokes equation can be derived from Eq. (23):

$$\rho\frac{\partial u}{\partial t} + \rho u\cdot\nabla u = -\nabla(c_{\mathrm{s}}^2\rho) + \nu\rho\nabla^2 u + F \quad (25)$$

where the kinetic viscosity

$$\nu = \frac{(2\tau - 1)}{6}\frac{\delta_x^2}{\delta_t}$$

and the speed of sound

$$c_{\mathrm{s}} = \frac{1}{\sqrt{3}}c$$

In the following analysis, we will consider only steady state flow satisfying

$$\frac{\partial u}{\partial x} = 0, \quad \frac{\partial v}{\partial x} = 0, \quad \text{and} \quad \rho = \text{const} \quad (26)$$

The body force is assumed to be along the x-direction, i.e., $F = \rho G i_x$, including external pressure-driven force and electro-viscous force due to electrokinetic potential. In this type of flow, both the velocity and the distribution functions are only functions of the y-coordinate. We define that the node $j = 0$ and $j = n$ corresponds to lower and upper boundaries, respectively, where the evolution rule depends on the implementation of boundary conditions. By substituting Eqs. (20) and (26) into Eq. (23) within the flow domain $(2 \leqslant j \leqslant n-2)$, the x-component of the momentum density ρu_j can be rewritten as

$$\begin{aligned}\rho u_j &= c\left[(f_1^j - f_3^j) + (f_5^j - f_6^j) + (f_8^j - f_7^j)\right] \\ &= \left[\frac{2}{3}\rho\Phi - \left(1 - \frac{2}{3}\Phi\right)\rho\frac{\tau - 1}{\tau} + \rho\frac{\tau - 1}{\tau}\frac{1 - \Phi}{\tau}\right]u_j \\ &\quad + \left[\frac{\rho\Phi}{6\tau} + \rho\frac{\tau - 1}{\tau}\left(1 - \frac{2}{3}\Phi\right)\right](u_{j+1} + u_{j-1}) \\ &\quad + \frac{\rho\Phi}{2\tau c}(u_{j-1}v_{j-1} - u_{j+1}v_{j+1}) + \frac{\delta_t\rho\Phi G}{\tau}\end{aligned} \quad (27)$$

For Poiseuille flow, the vertical velocity is zero and Eq. (27) can further reduce to

$$\begin{aligned}&\left[\left(\frac{4}{3}\Phi - 2\right)\tau + \left(1 - \frac{2}{3}\Phi\right) + \frac{\tau - 1}{\tau}(1 - \Phi)\right]u_j \\ &\quad + \left[\left(\frac{5}{6}\Phi - 1\right) + \tau\left(1 - \frac{2}{3}\Phi\right)\right](u_{j+1} + u_{j-1}) \\ &\quad + \frac{\delta_x\Phi G}{c} = 0\end{aligned} \quad (28)$$

where $\Phi = \exp(-U(x)/(k_{\mathrm{B}}T))$. By defining the following three parameters as

$$\begin{aligned}\Phi_1 &= \left(\frac{4}{3}\Phi - 2\right)\tau + \left(1 - \frac{2}{3}\Phi\right) + \frac{\tau - 1}{\tau}(1 - \Phi) \\ \Phi_2 &= \left(\frac{5}{6}\Phi - 1\right) + \left(1 - \frac{2}{3}\Phi\right)\tau \\ \Phi_3 &= \frac{\delta_x\Phi G}{c}\end{aligned}$$

Eq. (28) can be written as

$$\Phi_1 u_j + \Phi_2(u_{j+1} + u_{j-1}) + \Phi_3 = 0 \quad (29)$$

and the solution of Eq. (29) becomes

$$u_j = -\frac{\Phi_3 j(n - j)}{(\Phi_1 + 2\Phi_2)j(n - j) - 2\Phi_2} + U_{\mathrm{s}} \quad (30)$$

where U_{s} is the slip velocity depending on the implementation of the boundary condition for walls in a particular scheme. In order to find out the slip velocity, we need to apply Eq. (27) at the grid line next to the bottom wall $(j = 1)$ and the analysis for the top boundary is the same:

$$\Phi_1 u_1 + \Phi_2(u_0 + u_2) + \Phi_3 + (\tau - 1)(\tilde{\mathbf{u}}_{\mathbf{0}} - u_0) = 0 \quad (31)$$

where $\rho\widetilde{\mathbf{u}_0} = c\left[(f_1^0 - f_3^0) + (f_5^0 - f_6^0) + (f_8^0 - f_7^0)\right]$

f_5^0 and f_6^0 depend on the boundary condition implemented. Using Eqs. (30) and (31), we obtained the explicit expression for the slip velocity:

$$U_s = \frac{\Phi_3\left(\frac{\Phi_1(n-1)}{(\Phi_1+2\Phi_2)(n-1)-2\Phi_2} + \frac{\Phi_2(n-2)}{(\Phi_1+2\Phi_2)(n-2)-\Phi_2} - 1\right) - (\tau-1)(\widetilde{\mathbf{u}_0} - u_0)}{\Phi_1+\Phi_2} \tag{32}$$

By the modified bounce-back rule, we mean that collision and forcing still occur at boundary nodes. The pre-collision unknown distribution is set equal to the value of the distribution along the opposite direction:

$f_2^0 = f_4^0, \quad f_5^0 = f_7^0, \quad \text{and} \quad f_6^0 = f_8^0$

With the modified bounce-back rule, we can show that

$$U_s = \frac{\Phi_3\left(\frac{\Phi_1(n-1)}{(\Phi_1+2\Phi_2)(n-1)-2\Phi_2} + \frac{\Phi_2(n-2)}{(\Phi_1+2\Phi_2)(n-2)-\Phi_2} - 1 - \frac{2}{3}(\tau-1)\tau\right)}{\Phi_1+\Phi_2} \tag{33}$$

3.2. Model prediction and comparison with experimental results

To verify our theoretical analysis, we have further carried out numerical simulation for electrokinetic flow in microchannel. The dimensions of the microchannels were selected to be 5 mm in width and 30 mm in length; three microchannels of 14.1, 28.2 and 40.5 μm in height are also used. The choice of these parameters reflect our intention to compare the microchannel data reported by Ren et al. [43] as closely as possible. Such microfluidics flow can be described as a function of only the height-coordinate of the microchannel. If gravity effect is negligible, the body force F depends only on the externally applied pressure and the induced electrical field.

$$F = \rho G = \left(\frac{\mathrm{d}P}{\mathrm{d}x}\right)_{\mathrm{ext}} - |\rho_e E_x| \tag{34}$$

where ρ_e is the net charge density per unit volume at any point in the liquid; the electrokinetic potential E_x can be obtained through a balance between streaming current and electrical conduction current at steady state:

$$E_x = -\frac{\rho_e u(y)}{\lambda_0 + k\lambda_s} \tag{35}$$

where $u(y)$ is the velocity along the channel, λ_0 is the electrical conductivity of the liquid, and λ_s is the surface conductance.

The number of ion distribution in a symmetric electrolyte solution is of the Boltzmann distribution form:

$$\rho_e = -2ze \cdot n_0 \sinh\left(\frac{ze\psi}{k_B T}\right) \tag{36}$$

where ψ is the electrical potential at any point in the liquid, n_0 and z are the bulk ionic concentration and valence of ion, respectively, e is the charge of a proton, k_B is the Boltzmann constant and T is the absolute temperature.

To determine the electrokinetic potential E_x, the Poisson–Boltzmann equation and the equation of motion should be solved simultaneously. For the sake of simplicity, two approximate relations are employed to obtain the electrokinetic potential. The charge distribution in the solution is governed by the potential at the solid–liquid interface. The solution of the one-dimensional Poisson–Boltzmann equation for a specified boundary condition is

$$\psi = \begin{cases} \frac{2k_B T}{ze} \ln\left(\frac{1+\gamma\exp(-k_B j\delta_x)}{1-\gamma\exp(-k_B j\delta_x)}\right) & j\delta_x \leqslant H \\ \frac{2k_B T}{ze} \ln\left(\frac{1+\gamma\exp(-k_B (n-j)\delta_x)}{1-\gamma\exp(-k_B (n-j)\delta_x)}\right) & j\delta_x > H \end{cases} \tag{37}$$

where $\gamma = (\exp(ze\zeta/2k_B T) - 1)/(\exp(ze\zeta/2k_B T) + 1) = \tanh(ze\zeta/k_B T)$, ζ is the zeta potential at the shear plane, k is the Debye–Huckel parameter as $k^2 = 2z^2e^2n_0/\epsilon_r\epsilon_0 k_B T$, ϵ_r is the relative dielectric constant of the solution, ϵ_0 is the permittivity of vacuum and H is the half of height of a rectangular microchannel. The fully developed velocity profile for laminar is employed to determine the electrokinetic potential in a way that is computationally economical while retaining the basic behavior of the flow.

$$u(y) = \frac{4H^2}{2\mu}\left(\frac{\mathrm{d}P}{\mathrm{d}x}\right)_{\mathrm{ext}}\left[\left(\frac{j\delta_x}{2H}\right) - \left(\frac{j\delta_x}{2H}\right)^2\right] \tag{38}$$

By substituting Eqs. (36)–(38) into Eq. (35), we can obtain the body force term in the solution Eq. (30) of the 9-bit lattice Boltzmann single-relaxation-time model (Fig. 1), which will be used to study electrokinetic effect of liquid flow through a microchannel as the height is

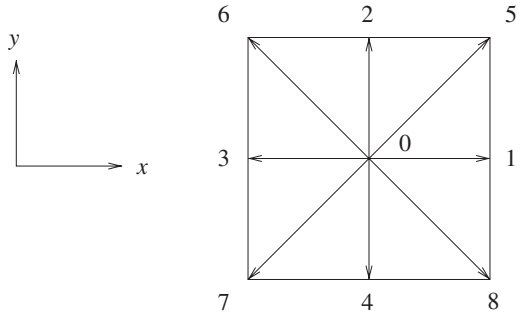

Fig. 1. Velocities of the 9-bit lattice model.

small in comparison with the channel width. The experimentally determined pressure gradients for the three different channel heights (14.1, 28.2 and 40.5 μm) and three electrolyte solutions (de-ionized ultra-filtered water (DIUF), aqueous KCl solution of 10^{-4} and 10^{-2} M concentrations) were applied to our model to predict the Reynolds numbers. Since these data were not tabulated, we digitized the experimental results in [43] to the best of our ability and reproduced them here. Other input parameters for the solutions and channel were obtained from [43]. The Reynolds number was calculated from

$$Re = \frac{\rho u_{\mathrm{m}} D_{\mathrm{h}}}{\mu}$$

where $D_{\mathrm{h}} = 4HW/(H+W)$ is the hydraulic diameter of the rectangular channel of width $2W$, height $2H$; u_{m} is the mean velocity and μ is the dynamic viscosity of the liquid. According to the lattice Boltzmann model, the kinetic viscosity can be expressed as

$$v = \frac{2\tau - 1}{6}\frac{\delta_x^2}{\delta_t}$$

To ensure the above kinetic viscosity from the lattice Boltzmann model is as consistent as the measured value v_{exp}, we obtain the lattice constant from

$$\delta_x = \frac{6v_{\mathrm{exp}}}{(2\tau - 1)c}$$

The only remaining parameter is the dimensionless relaxation time $\tau(\tau > 0.5)$, which represents the interparticle interactions of a given system and was adjusted to fit the results. The model predictions together with the experimental data are shown in Tables 1–3 and in Figs. 2–4. It is apparent that the predicted Reynolds numbers *Re* are in excellent agreement with those determined experimentally for the three electrolyte solutions in different channel sizes. With respect to the 40.5 μm channel in Table 3, we were not able to distinguish the experimental data between the cases for DIUF water, 10^{-2} and 10^{-4} M of KCl solutions. Thus, only one set of experimental data was reported in Table 3 and compared against three sets of model results. The predictions from 9-bit square lattice Boltzmann model agree very well with the experimental data. The differences between the

Table 1
Comparison of the experimental values for dP/dx versus *Re* in Ref. [43] with the predictions from the lattice Boltzmann analytical model for a microchannel of 14.1 μm in height using 10^{-2} M KCl solution, 10^{-4} M KCl solution and DIUF water

dP/dx (10^6 Pa/m)	*Re* [43]	*Re* (Predicted)
10^{-2} M KCl solution		
1.93	1.00	0.93
2.60	1.31	1.26
3.32	1.52	1.61
3.82	1.79	1.85
10^{-4} M KCl solution		
2.28	1.04	0.98
3.04	1.29	1.30
3.60	1.54	1.54
4.29	1.85	1.84
DIUF water		
2.35	0.98	0.95
3.08	1.28	1.25
3.71	1.52	1.51
4.43	1.79	1.80

Table 2
Comparison of the experimental values for dP/dx versus *Re* in Ref. [43] with the predictions from the lattice Boltzmann analytical model for a microchannel of 28.2 μm in height using 10^{-2} M KCl solution, 10^{-4} M KCl solution and DIUF water

dP/dx (10^6 Pa/m)	*Re* [43]	*Re* (Predicted)
10^{-2} M KCl solution		
2.32	8.62	8.27
2.82	10.77	10.06
3.39	12.92	12.09
3.89	15.15	15.25
4.45	17.38	17.45
10^{-4} M KCl solution		
2.58	8.62	8.72
3.08	10.77	10.42
3.58	12.92	12.11
4.08	15.15	15.06
4.58	17.38	16.91
DIUF water		
2.68	8.62	8.44
3.16	10.77	9.96
3.69	12.92	12.71
4.18	15.15	14.76
4.71	17.38	16.64

Table 3
Comparison of the experimental values for dP/dx versus Re in Ref. [43] with the predictions from the lattice Boltzmann analytical model for a microchannel of 40.5 μm in height using 10^{-2} M KCl solution, 10^{-4} M KCl solution and DIUF water

dP/dx (10^6 Pa/m)	Re[a] [43]	Re (Predicted)		
		10^{-2} M KCl	10^{-4} M KCl	DIUF water
1.64	16.92	16.69	16.93	16.97
2.05	21.15	20.86	21.17	21.22
2.36	25.00	24.01	24.37	24.43
3.14	33.46	34.05	32.43	32.51
3.86	41.92	41.86	39.86	41.15
4.64	50.77	50.31	49.13	49.46
5.31	59.00	58.73	56.95	57.78

[a] We reported here only one set of data because the experimental data in [43] for the three liquids appear to be the same.

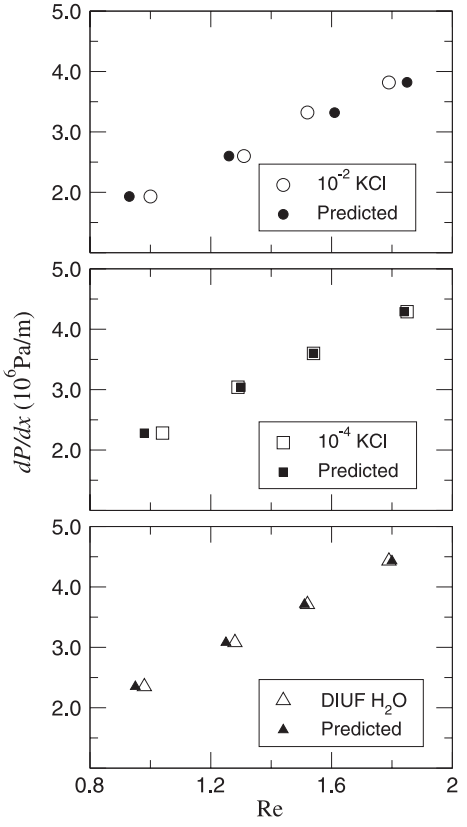

Fig. 2. Comparison of the experimentally determined dP/dx versus Re relationships in Ref. [43] with the predictions from the 9-bit square lattice Boltzmann model for a microchannel of 14.1 μm in height.

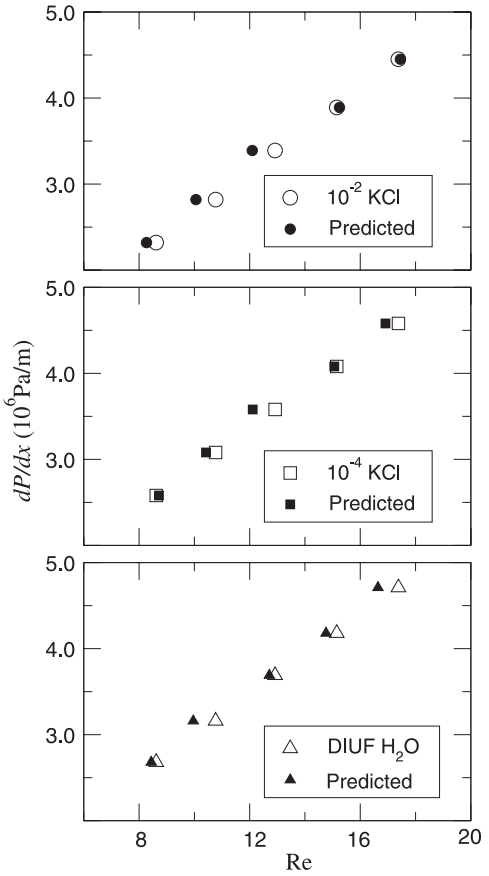

Fig. 3. Comparison of the experimentally determined dP/dx versus Re relationships in Ref. [43] with the predictions from the 9-bit square lattice Boltzmann model for a microchannel of 28.2 μm in height.

predicted and experimental values are well within 5% for the systems studied. The lattice Boltzmann model in the presence of external force presented in this paper is an effective computational tool for complex microfluidic systems that might be problematic using conventional methods.

4. Summary

We have derived a lattice Boltzmann model in the presence of external forces for microfluidics with

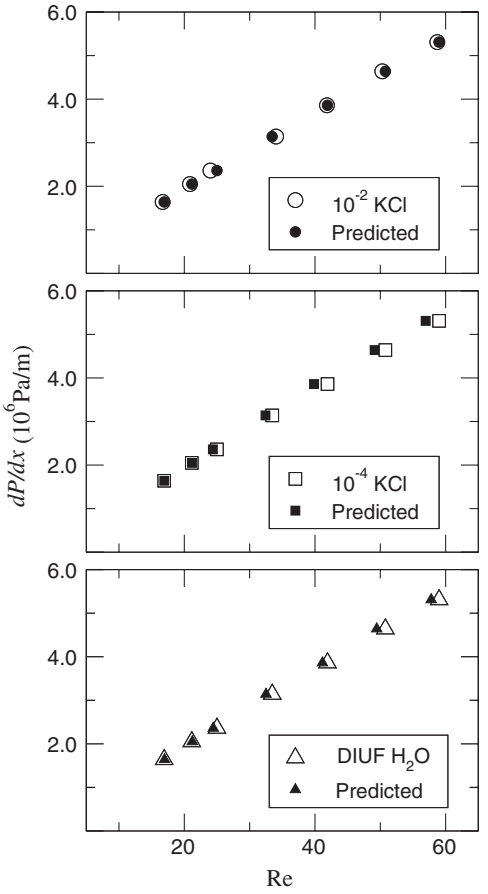

Fig. 4. Comparison of the experimentally determined dP/dx versus *Re* relationships in Ref. [43] with the predictions of the 9-bit square lattice Boltzmann model for a microchannel of height 40.5 μm.

electrokinetic phenomena. The external force field considered here is the applied external pressure for liquid flow. Excellent agreement was found between the results from our 9-bit square lattice Boltzmann model and those from recent experimental data for pressure-driven microchannel flow of electrolyte solutions. The lattice Boltzmann model established here is shown to be an effective computational tool for more complex microfluidic systems that could not be described by conventional approaches.

Acknowledgements

We gratefully acknowledge financial support from the Alberta Ingenuity Establishment and Student Funds, Canada Research Chair (CRC) Program, Canada Foundation for Innovation (CFI), Petro-Canada Young Innovator Fund, and Natural Sciences and Engineering Research Council of Canada (NSERC) in support of this research.

References

[1] Y.J. Song, T.S. Zhao, J. Micromech. Microeng. 11 (2001) 713.
[2] J.N. Pfrahler, A. Bar-Cohen, A.D. Kraus, Advances in thermal modeling of electronic components and systems, vol. II, ASME Press, New York, 1990 (Chapter 3).
[3] C.E. Hunt, C.A. Desmond, D.R. Ciarlo, W.J. Benett, J. Micromech. Microeng. 1 (1991) 152.
[4] J.D. Harrison, K. Fluri, K. Seiler, Z.H. Fan, C.S. Effenhauser, A. Manz, Science 261 (1993) 895.
[5] P.J. Blackshear, Sci. Am. 241 (1979) 52.
[6] R.D. Penn, J.A. Paice, W. Gottschalk, A.D. Ivankovich, J. Neurosurg. 61 (1984) 302.
[7] J. Lyklema, in: Fundamentals of Interface and Colloid Science, vol. II, Academic Press, 1995.
[8] J. Yang, D.Y. Kwok, J. Chem. Phys. 118 (2003) 354.
[9] J. Yang, D.Y. Kwok, J. Phys. Chem. B 106 (2002) 12851.
[10] J. Yang, D.Y. Kwok, J. Colloids Interface Sci. 260 (2003) 225.
[11] J. Yang, D.Y. Kwok, Langmuir 19 (2003) 1047.
[12] J. Yang, D.Y. Kwok, J. Micromechan. Microeng. (2002).
[13] J.F. Zhang, D.Y. Kwok, J. Phys. Chem. B 106 (2002) 12594.
[14] S.-W. Lee, D.Y. Kwok, P.E. Laibinis, Phys. Rev. E 65 (2002) 051602.
[15] H. Greberg, R. Kjellander, J. Phys. Chem. 108 (1998) 2940.
[16] E. González-Tovar, M. Lozada-Cassou, W. Olivares, J. Chem. Phys. 94 (1991) 2219.
[17] W. Olivares, B. Sulbarán, M. Lozada-Cassou, J. Phys. Chem. 97 (1993) 4780.
[18] W. Olivares, B. Sulbarán, M. Lozada-Cassou, J. Chem. Phys. 103 (1995) 8179.
[19] P. Zaini, H. Modarress, G.A. Mansoori, J. Chem. Phys. 104 (1996) 3832.
[20] B. Li, D.Y. Kwok, Phys. Rev. Lett. 90 (2003) 124502.
[21] G. McNamara, G. Zanetti, Phys. Rev. Lett. 61 (1988) 2332.
[22] G.D. Doolen, Lattice Gas Methods for Partial Differential Equations, second ed., Addison-Wesley, 1991.
[23] G.D. Doolen, Lattice Gas Methods: Theory, Applications and Hardware, second ed., MIT, 1991.
[24] H. Chen, S. Chen, W.H. Matthaeus, Phys. Rev. A 45 (1991) R5339.
[25] D.P. Lockard, L.S. Luo, S.D. Milder, B.A. Singer, J. Stat. Phys. 107 (1/2) (2002) 423.
[26] D. d'Humieres, I. Ginzburg, M. Krafczyk, P. Lallemand, L.-S. Luo, Proc. Royal Soc. London A 260 (1792) (2002) 437.
[27] X. Shan, H. Chen, Phys. Rev. E 47 (1993) 1815.
[28] X. Shan, G. Doolen, J. Stat. Phys. 81 (1995) 379.
[29] S. Chen, H. Chen, D. Martinez, W. Matthaeus, Phys. Rev. Lett. 67 (1991) 3776.
[30] X. Shan, H. Chen, Phys. Rev. Lett. 49 (1994) 2941.
[31] M.R. Swift, W.R. Osborn, J.M. Yeomans, Phys. Rev. Lett. 75 (1995) 830.
[32] A.J.C. Ladd, J. Fluid Mech. 271 (1994) 285.

[33] B.M. Boghosian, P.V. Coveney, A.N. Emerton, Proc. Royal Soc. Ser. A 452 (1996) 1221.
[34] R. Mei, D. Yu, W. Shyy, L.S. Luo, Phys. Rev. E 65 (4) (2002) 041203.
[35] M. Bouzidi, D. d'Humieres, P. Lallemand, L.S. Luo, J. Comput. Phys. 172 (2001) 704.
[36] L.S. Luo, Phys. Rev. E 62 (4) (2002) 4982.
[37] X. He, L.S. Luo, Phys. Rev. E 56 (6) (1997) 6811.
[38] X. He, L.S. Luo, Phys. Rev. E 55 (2002) R6333.
[39] X. He, L.S. Luo, J. Stat. Phys. 88 (1997) 927.
[40] X. He, Q. Zou, L.S. Luo, M. Dembo, J. Stat. Phys. 87 (1997) 115.
[41] X. He, X. Shan, G.D. Doolen, Phys. Rev. E 57 (1) (1998) 13.
[42] B. Li, D.Y. Kwok, Langmuir 19 (2003) 3041.
[43] L. Ren, W. Qu, D. Li, Int. J. Heat Mass Transfer 44 (2001) 3125.